# Weathering of ultramafic rocks and element mobility at Mt. Prinzera, Northern Apennines, Italy

GIAMPIERO VENTURELLI, SIMONA CONTINI*, ACHILLE BONAZZI

Dipartimento di Scienze della Terra, Università di Parma, Viale delle Scienze 78, 43100 Parma, Italy

AND

ALESSANDRO MANGIA

Dipartimento di Chimica Generale e Inorganica, Università di Parma, Viale delle Scienze 78, 43100 Parma, Italy

## Abstract

The weathering of the Mt. Prinzera serpentinites (Parma province, Northern Apennines, Italy) produced dominant smectite and minor Fe-hydroxides. The mobility of the elements during weathering has been estimated using the ratio $K_i = M_i^S/M_i^R$, where $M_i$ indicates the mass of a generic component $i$ before ($R$) and after ($S$) the weathering, and using $TiO_2$ as a practically immobile component. For prevalently to tendentially mobile elements, the degree of mobility, which in our case increases as $K_i$ decreases, is in the order Mn $\approx$ Cr = Fe < V $\approx$ Zn $\approx$ Co < Ni < Si < Mg < Ca. The elements Ti, Ga, Al and Zr are prevalently immobile. The mass chemically removed by the circulating waters during weathering may reach very high values (on average 52% of the original mass of serpentinite) and the main contribution to the mass loss is due to Si and Mg. The composition of the perennial and ephemeral springs in the area is in agreement with the degree of the element mobility at least for Cr, Mg and Ca.

KEYWORDS: element mobility, weathering, serpentinites, Northern Apennines, Italy.

## Introduction

THE ultramafic rocks of the Northern Apennines (Italy) are prevalently lherzolite tectonites and belong to an ophiolite sequence which represents remnants of a Mesozoic oceanic area (Piccardo *et al.*, 1990; Rampone *et al.*, 1993, and references therein). The ultramafic rocks underwent variable degree of serpentinization, mostly in an oceanic environment: lizardite is the prevalent serpentine polytype formed during this process, whereas chrysotile is only accessory. According to Beccaluva *et al.* (1973), among Ca, Fe, Mg, Mn, Cr, Ni and Co, only Ca appears clearly mobilized during serpentinization.

Geochemical and mineralogical studies on weathering affecting ultramafic rocks and related element mobility are present in the literature (e.g. Barnes and O'Neil 1969; Wildman *et al.*, 1971; Wilson and Berrow, 1978; Nahon and Colin, 1982; Shellmann, 1989*a,b*, and references therein). Similar investigations, however, are practically absent in the Apennines; thus this study deals with weathering of some ultramafic rocks of the Northern Apennines (Mt. Prinzera, Parma province) and consists of: (1) a description of the mineralogy related to the weathering of the ultramafic substratum; (2) general considerations about element mass-balance during the weathering and a geochemical investigation on the weathering process and element mobility.

## Climate

According to the data referred to for the period 1917–1975, in the area, the average precipitation is

* Present address: GEODE SCRL-Studi Geologici e Petrografici, Viale Duca Alessandro 1, 43100 Parma, Italy.

*Mineralogical Magazine, December 1997, Vol. 61, pp. 765–778*

about 950 mm $yr^{-1}$, with the highest levels in November and April (103 and 91 mm $month^{-1}$ respectively) and the lowest level in July and January (34 and 66 respectively). No data are available on the chemical-physical features of the rain at Mt. Prinzera; however, starting from 1989, data have been systematically collected for neighbouring areas. The pH of the rain (G. Curti, pers. comm. 1995) is usually in the range 4.2–7.0 (average 5.1): lower values have been occasionally recorded in the town of Parma (3.6); higher values (up to 8) have been recorded at the end of May 1994 in concomitance with cloud systems coming from North Africa and probably carrying calcareous dust. During January and July, the average temperature reaches the lowest (from about 4 to about −6°C) and the highest (from about 28 to about 16°C) values respectively.

## The ultramafic rocks of Mt. Prinzera (44°38′30″N, 10°5′ E)

*Field geology.* Mt. Prinzera is located about 35 km SW of the town of Parma (Emilia Romagna Region) and consists of serpentinized mantle tectonites which cover an area of about 0.8 $km^2$. The ultramafic rocks, which in places exhibit foliation, rest on Lower Cretaceous dark shales and limestones, Palaeocene flysch (calcite, quartz, muscovite, biotite, chlorite, feldspar), and Cretaceous shales (illite and smectite, quartz and probable kaolinite, gibbsite and dolomite in minor amounts). At the bottom of the ultramafic body, tectonic peridotite breccias are common; they are strongly altered and oxidized and are frequently cut by a network of calcite veins. The lowest part of the body consists locally of an altered polygenic breccia which includes serpentinite fragments, clasts of limestone and fragments of calcite veins, and probably represents the relics of an olistostrome. The alteration of the breccias is related to low-temperature hydrothermal activity which probably occurred on the sea-floor.

*Pre-weathering mineralogy.* The pre-serpentinization assemblage includes, in decreasing amounts: olivine (Mg# = 100 × Mg/(Mg+Fe), atomic ratio, 90.0–90.5); orthopyroxene (Mg# ≈ 90); clinopyroxene (Mg# ≈ 91) as main components; Cr-Al-spinel, plagioclase, armouring spinel, and calcic-sodic amphibole as accessory phases (Table 1).

The serpentinization related to oceanic (and orogenic?) metamorphism generated serpentine (lizardite and rare chrysotile), and minor chlorite, magnetite and sulphide. Most goethite and Mn-rich oxide, calcite and in part smectite and probable mixed layer smectite-chlorite (Table 2) represent products of hydrothermal activity at lower temperature. Lizardite, which has been identified on the basis of typical diffractions at ≈ 2.49, 1.53 and 1.50 Å, developed from fractures and cleavage planes of the Mg-Fe-silicates and constitutes a continuous network. Chrysotile, distinguished from lizardite on the basis of the diffraction at 2.45 Å, occupies late narrow veins (usually < 0.2 mm wide; Fig. 1A) and consists of fibres disposed normally to

TABLE 1. Composition of pre-serpentinization minerals

| | Olivine | Opx | Cpx | Amph | Spinel |
|---|---|---|---|---|---|
| wt.% | | | | | |
| $SiO_2$ | 40.2 | 55.7 | 51.5 | 42.3 | |
| $TiO_2$ | 0.09 | 0.25 | 0.26 | 5.04 | 0.34 |
| $Al_sO_3$ | | 1.73 | 6.25 | 12.9 | 40.7 |
| $FeO_{tot}$ | 9.17 | 6.65 | 2.55 | 4.15 | 18.3 |
| MnO | | 0.11 | | | |
| MgO | 48.9 | 34.9 | 15.4 | 16.2 | 14.7 |
| CaO | | 0.39 | 20.7 | 11.8 | |
| $Na_2O$ | | 0.19 | 1.68 | 3.39 | |
| $K_2O$ | | | | 0.10 | |
| $Cr_2O_3$ | | | 1.08 | 1.46 | 24.1 |
| Total | 98.36 | 99.92 | 99.42 | 97.34 | 98.14 |
| Mg# | 90 | 90 | 91 | 87 | |

Opx = orthopyroxene, Cpx = clinopyroxene, Amph = calcic-sodic amphibole, Mg# = 100 × Mg/(Mg+Fe), atomic ratio. Analyses performed by Jeol 6400/Tracor EDS microanalysis: operating conditions 15 kV, 0.62 nA.

TABLE 2. Representative analyses of some secondary minerals

| | Serpentine | | | Chlorite | | | | | | | | | Sm-Chl | | Oxides/hydroxide | |
|---|---|---|---|---|---|---|---|---|---|---|---|---|---|---|---|---|
| | 1 | 2 | 3 | 4 | 5 | 6 | 7 | 8 | 9 | 10 | 11 | 12 | 13 | 14 | 15 | 16 |
| wt.% | (am) * | (opx) | | (pl) | (am) | (opx) | | | (sulph) | (sulph) | | | | | | ** |
| $SiO_2$ | 39.3 | 39.6 | 40.1 | 33.0 | 33.2 | 29.6 | 31.1 | 34.5 | 26.4 | 27.2 | 29.0 | 29.8 | 40.5 | 39.2 | 1.41 | 7.21 |
| $Al_2O_3$ | 3.52 | 1.98 | 0.90 | 11.4 | 12.8 | 18.9 | 13.4 | 0.90 | 15.1 | 12.1 | 17.3 | 14.6 | 1.50 | 2.09 | | 1.21 |
| $FeO_{tot}$ | 4.22 | 5.46 | 4.21 | 9.64 | 10.4 | 9.78 | 13.4 | 22.2 | 36.6 | 36.3 | 22.4 | 26.5 | 18.6 | 19.6 | 89.8 | 2.10 |
| MnO | 0.20 | | 0.79 | | 0.19 | 0.60 | 0.20 | 0.18 | 0.28 | 0.45 | 0.96 | 0.56 | | | 1.61 | 47.8 |
| MgO | 37.9 | 39.2 | 39.2 | 27.4 | 27.2 | 27.4 | 26.7 | 22.4 | 8.20 | 8.34 | 19.2 | 17.0 | 22.2 | 21.5 | 0.89 | 12.5 |
| CaO | 0.10 | | | 1.30 | 0.88 | 0.58 | 0.38 | 0.19 | 0.52 | 0.35 | 0.28 | 0.46 | 0.68 | 0.71 | 0.22 | 1.23 |
| $Na_2O$ | | | | 0.40 | 0.55 | 0.26 | 0.25 | 0.25 | | 0.40 | 0.35 | 0.29 | 0.20 | 0.60 | | |
| NiO | 0.15 | | 0.20 | | 0.19 | 0.23 | | | 0.55 | | | | | 0.08 | | 2.85 |
| Total | 85.79 | 86.24 | 85.40 | 83.14 | 85.41 | 87.35 | 85.43 | 80.62 | 87.65 | 85.14 | 89.49 | 89.21 | 83.68 | 83.78 | 93.93 | 75.18 |
| Cations | | | | | | | | | | | | | | *** | | *** |
| Si | 3.788 | 3.805 | 3.883 | 3.376 | 3.319 | 2.894 | 3.162 | 3.922 | 2.991 | 3.181 | 2.955 | 3.110 | 4.256 | 3.344 | 4.160 | 3.268 |
| Al | 0.400 | 0.224 | 0.103 | 1.375 | 1.508 | 2.178 | 1.606 | 0.121 | 2.017 | 1.668 | 2.078 | 1.796 | 0.186 | 0.146 | 0.261 | 0.205 |
| $Fe^{2+}_{tot}$ | 0.340 | 0.439 | 0.341 | 0.825 | 0.869 | 0.800 | 1.139 | 2.111 | 3.468 | 3.550 | 1.909 | 2.313 | 1.635 | 1.284 | 1.739 | 1.367 |
| Mn | 0.016 | | 0.065 | | 0.016 | 0.050 | 0.017 | 0.017 | 0.027 | 0.045 | 0.083 | 0.050 | | | | |
| Mg | 5.445 | 5.614 | 5.658 | 4.178 | 4.052 | 3.992 | 4.045 | 3.795 | 1.385 | 1.453 | 2.916 | 2.644 | 3.477 | 2.732 | 3.400 | 2.671 |
| Ca | 0.010 | | | 0.142 | 0.094 | 0.061 | 0.041 | 0.023 | 0.063 | 0.044 | 0.031 | 0.051 | 0.077 | 0.060 | 0.081 | 0.063 |
| Na | | | | 0.079 | 0.107 | 0.049 | 0.049 | 0.055 | | 0.091 | 0.069 | 0.059 | 0.041 | 0.032 | 0.123 | 0.097 |
| Ni | 0.012 | | 0.016 | | 0.015 | 0.018 | | | 0.050 | | | | | | 0.007 | 0.005 |
| Mg# | 94 | 93 | 94 | 83 | 82 | 83 | 78 | 64 | 28 | 29 | 60 | 53 | 68 | | 66 | |

Sm-Chl = probable mixed layer smectite-chlorite; ( ) parental phases: am = calcic-sodic amphibole, opx = orthopyroxene, pl = plagioclase, sulph = sulphide; *, includes 0.40 % $TiO_2$; **, includes 0.28 % $TiO_2$; 1–2 = network-forming serpentine; 3 = vein; 4–7 = pennine; 8 = diabantite; 9–10 = brunsvigite; 11 = pycnochlorite; 12 = low-silica diabantite; 15 = magnetite associated with lizardite; 16 = Ni-rich manganese hydroxide. ***, cations on the basis of 11 equivalent oxygens; for the other cases, cations on the basis of 14 equivalent oxygens.

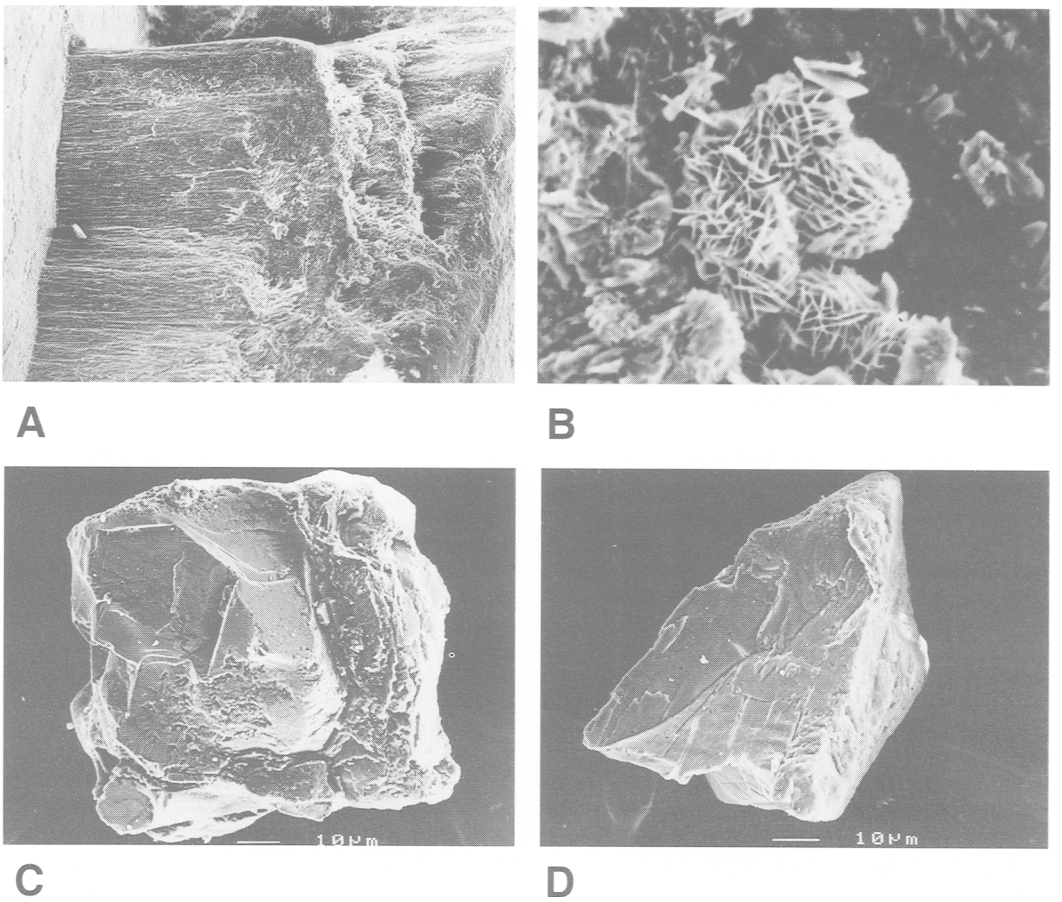


FIG. 1. SEM images of minerals occurring in serpentinitic rocks and related soil. (A) Chrysotile vein between lizardite walls in serpentinite (width of view ≈ 500 µm). (B) Aggregates of goethite located along fractures in strongly oxidized serpentinite (width of view ≈ 45 µm). (C) Grain of relict spinel in soil: the grain exhibits dissolution microcavities (width of view ≈ 130 µm). (D) Grain of quartz in soil (width of view ≈ 130 µm).

the walls of the veins. Several kinds of chlorites have been identified as indicated in Table 2 (nomenclature according to Hey, 1954). A late yellow–brown phase occasionally occurring mostly in the inner portions of serpentine veins (analyses 13, 14) could represent an association of small separated domains of chlorite and smectite (≪ 2 µm, the approximate maximum size of the electron spot during analysis) or mixed layer smectite-chlorite after previous chlorite. Also observed was Mn-bearing magnetite (analysis 15) which forms euhedral crystals associated with lizardite. Small veins of brown-black Mn-rich, Ni-bearing hydroxides may cut previous secondary phases.

## Mineralogy of the weathering products

### *General*

The ultramafic rocks are partly covered by weathering products (soil/saprolite) which, in places, underwent transport and local accumulation. Vegetation is scarcely developed. The investigated samples of soil/saprolite, came from nine profiles and from two other localities, as listed in Table 3 together with the main mineralogical features of the samples. Each sample represents about 1–2 $dm^3$ of weathered material. Number 27A refers to a hydrothermally transformed and strongly oxidized serpentinite breccia; number 27 to a soil accumulated mostly from material 27A.

TABLE 3. Profiles and sampled weathering products

| Sample | Depth (cm) | pH | Bulk sample mineralogy | | | | | Fraction < 2 μm |
|---|---|---|---|---|---|---|---|---|
| | | | Serp | Clay minerals | Chl | Qtz | Fsp | Clay type |
| Station 1 | | | | | | | | |
| PR21 | 0–10 | 7.3 | +++ | + | – | + | – | Sm |
| PR20 | | 7.5 | +++ | + | – | – | – | Sm |
| Station 2 | | | | | | | | |
| PR19 | 0–5 | 7.2 | +++ | + | + | tr | tr | Sm+Chl |
| PR18(1) | 5–20 | 7.2 | +++ | + | + | tr | – | Sm+Chl |
| PR18(2) | 20–30 | 7.4 | +++ | + | + | + | – | Sm+Chl(*) |
| PR17 | 30–55 | 7.6 | +++ | + | + | + | – | Sm+Chl |
| Station 3 | | | | | | | | |
| PR16(1) | 0–15 | 7.2 | +++ | ++ | + | tr | – | Sm+Chl |
| PR16(2) | 15–20 | 7.4 | +++ | + | + | + | – | Sm(*) |
| PR15 | 20–50 | 7.8 | ++ | ++ | – | + | tr | Sm(*) |
| PR14 | | 7.3 | | | | | | Sm |
| Station 4 | | | | | | | | |
| PR47 | 0–20 | 7.1 | +++ | + | + | + | – | Sm+Chl(*) |
| PR46 | 20–50 | 7.0 | +++ | ++ | + | + | tr | Sm(*) |
| PR45 | | 7.3 | +++ | + | – | – | – | Sm(*) |
| Station 5 | | | | | | | | |
| PR51 | 0–25 | 6.7 | +++ | + | – | + | – | Sm |
| PR50 | 25–60 | 6.8 | +++ | + | + | + | – | Sm |
| Station 6 | | | | | | | | |
| PR54 | 0–25 | 6.9 | +++ | + | – | + | – | Sm |
| PR53 | 25–50 | 7.1 | +++ | + | – | + | tr | Sm |
| PR52 | | 7.0 | +++ | + | + | + | tr | Sm |
| Station 7 | | | | | | | | |
| PR60 | 0–35 | 6.8 | +++ | + | + | + | + | Sm |
| PR61 | | 6.4 | +++ | + | + | + | tr | Sm |
| Station 8 | | | | | | | | |
| PR41 | 0–10 | | + | +++ | + | + | – | Sm |
| PR43 | 10–35 | | + | +++ | – | + | – | Sm |
| PR44 | 35–60 | | + | +++ | + | – | – | Sm |
| PR55 | 60–80 | 7.2 | ++ | ++ | + | + | – | Sm |
| PR56 | | 7.1 | ++ | ++ | + | + | – | Sm |
| Station 9 | | | | | | | | |
| PR59 | 0–5 | 6.9 | +++ | + | – | + | tr | Sm+Chl(*) |
| PR58(2) | 20–40 | 6.8 | ++ | ++ | – | + | tr | Sm+Chl(*) |
| PR57 | | 6.6 | ++ | ++ | – | + | – | Sm |
| Station 10 | | | | | | | | |
| PR27 | | 7.0 | – | +++ | – | tr | – | Sm(*) |
| Hydrothermal | | | | | | | | |
| PR27A | | 7.7 | + | +++ | – | tr | – | Sm |

Srp = serpentine; Chl = chlorite; Qtz = quartz; Fsp = feldspars; Sm = smectite; (*) = occurrence of peak in the range 11–12 Å in heated samples; tr = trace. Sample PR027 exhibits significant amounts (some per cent) of hematite and goethite and represents a soil generated by accumulation of clay and oxides-hydroxides prevalently coming from hydrothermal rock PR27A. Sample PR27A contains abundant calcite veins and minor hematite and goethite (some per cent). X-ray diffaction data obtained using a goniometer Philips, Cu Kα and CoKα radiations and silicon as internal standard. The pH of the soil samples has been determined by standard procedure, i.e. after mixing rock and deionized water in mass proportion 1/2.5, shaking for about 10 minutes and one hour of resting.

In addition to relics of minerals belonging to the pre-serpentinization paragenesis (pyroxenes, spinel and olivine), the mineral assemblage of the soil includes lizardite, clays, Fe-oxides/hydroxides (e.g. Fig. 1B), chlorite, quartz, plagioclase, K-feldspar, calcite and exceptional zircon, biotite, epidote and dolomite. With the exception of lizardite, smectitic minerals and Fe-oxides/hydroxides, the other phases are present in low to very low amounts. Lizardite and chlorite represent relics of serpentinite. Frequently the minerals such as relic olivine, spinel (Fig. 1C) and lizardite exhibit microcavities which are interpreted as being generated by dissolution.

The different species of clay minerals have been identified by XRD on the fraction with conventional diameter < 2 μm according to a standard procedure (Thorez, 1976). All the natural samples dried at 30°C exhibit a main diffraction in the range 14.3–15.8 Å, which may be asymmetrically developed at low angle; after glycolation, the peak shifts to 16.6–18 Å or may split into two peaks at about 14 and 17 Å. After heating to 500°C, three main groups of samples may be distinguished: (1) usually the spacing is reduced to 9.7–10 Å suggesting that only smectite was present; (2) in addition to the diffractions at about 10 Å, a peak at 13.8–14.3 Å may also occur in agreement with the presence of both smectite and chlorite; (3) rarely a small peak in the range 10.5–11.8 Å is present in addition to the 10 Å peak. Case (3) could suggests the occurrence of mixed layer smectite-chlorite in addition to smectite. It is noteworthy that mixed layer smectite-chlorite has been hypothesized in soil derived from the ophiolite of Serra Zanchetto (Bologna province: Minguzzi *et al.*, 1985).

*Allogenic minerals.* As summarized in Table 3, the investigated samples may contain some quartz. Quartz has been found elsewhere in soil derived from ultramafic rocks and interpreted in different ways (e.g. Cleaves *et al.*, 1974; Cortesogno *et al.*, 1976; Wilson and Berrow, 1978; Yusta *et al.*, 1985; Shellmann, 1986*b*). For instance, Cleaves *et al.* (1974) and Shellmann (1986*b*) assumed that quartz is of secondary origin; Wilson and Berrow, (1978) and Yusta *et al.* (1985) suggested an allogenic nature.

Hypotheses on the origin of quartz at Mt. Prinzera must explain the following observations: (1) quartz in the altered ultramafic fragments of the soil/saprolite or quartz coating these fragments has not been found; (2) the examined quartz grains never exhibit euhedral habit; (3) a comparison with morphological data reported in the literature (Pittman 1972, Mazzullo *et al.*, 1984, and references therein) indicates that the quartz grains do not exhibit overgrowth but rather incipient dissolution (Fig. 1D). All these features are evidence against a secondary origin of quartz during dissolution of silicates and indirectly supports an allogenic nature for this mineral. The same origin must be attributed to other phases, such as K-feldspar, biotite and zircon, which cannot form by alteration of ultramafic rocks. It is reasonable to suggest that the allogenic minerals were accumulated by aeolian or surface water transport from surrounding sedimentary formations and/or from areas further afield.

The sample fraction with conventional diameter <2 μm does not exhibit quartz diffractions suggesting that this mineral is absent or present in very low amounts in this portion. Hypotheses which may explain this feature are: (1) surface water circulating in the soil removed the smallest quartz fractions downwards; (2) the small grains were more easily dissolved than the large ones (3) in nature it is difficult to comminute quartz to size <2 μm.

Process (1) would lead to an increasing quartz concentration in the lowest weathered levels; however, the different soil levels do not exhibit any systematic variation in quartz proportion suggesting that accumulation of quartz downward did not act significantly.

Hypothesis (2) needs more detailed comments. It is well known that solubility of a phase may depend in variable extent on the grain size as small crystals are thermodynamically less stable. The relationship between activity of the component in water and crystal size (e.g. Enüstün and Turkevich, 1960; Stumm and Morgan, 1981) at defined $T$ and $P$ under equilibrium conditions, is defined in the following expression:

$$\log(a/a_0) = \frac{(2/3)M\alpha\gamma}{2.303RTDx} \qquad (1)$$

where: M = formula weight of the phase, $\alpha$ = characteristic geometric factor depending on the grain shape, $\gamma$ = mean interfacial tension, D = density of the phase, $x$ = characteristic dimension of the grains, T = absolute temperature, R = gas constant, $a$ = activity of the dissolved component, $a_o$ = activity of the component when the grain size is very large ($x \rightarrow \infty$). Equation (1) may be used to calculate the relative variation of activity, $(a/a_o) - 1$, for different values of the grain dimension. For example, considering that M = 60.09, D = 2.65 g cm$^{-3}$ and $\gamma$ = 0.35 Jm$^{-2}$ (Parks, 1984) and assuming spherical granules ($\alpha = 6$) and T = 25°C, we obtain that only the solubility of grains with diameter $\leqslant$ 0.13 μm exceeds the solubility of macrocrystalline quartz of a value $\geqslant$10% ($(a/a_o)-1 \geqslant 0.10$); significant excess of solubility for grain sizes up to 2 μm could only be obtained considering very high $\alpha$ values. Thus we conclude that variation of thermodynamic parameters dependent on grain size cannot be the main reason of the practical absence or very low content of quartz in the fraction <2 μm.

The grain size, however, could influence the rate of crystal dissolution. The rate of dissolution via molecular diffusion (cf. Nielsen, 1964; Berner, 1981) may be given by the following approximate expression:

$$\frac{dx}{dt} \propto \frac{(C_\infty - C_{eq})}{x} \qquad (2)$$

where: $x$ = characteristic dimension of the grain, $C_\infty$ = concentration in solution away from the crystal surface, $C_{eq}$ = equilibrium concentration adjacent to the crystal surface, t = time. Equation (2) indicates that, in agreement with hypothesis (2) the rate of dissolution dx/dt increases with decreasing grain dimension.

Finally, hypothesis (3) cannot be proved or disregarded, but only accepted as a possibility supported by the absence of quartz in the clay-size fraction of recent glacial outwash in Alaska and in pedogenetically unweathered glacial tills (Drees *et al.*, 1989, and references therein).

### Introduction to mass-balance and definitions

*General.* Reliable information on element mobility during weathering may be obtained by a quantitative mass-balance approach as reported below. Consider a volume $V^R$ of a rock $R$ with density $D^R$, total mass $M^R$ and mass $M_i^R$ of the chemical component $i$; by exchenge of chemical components with the environment, the original rock is transformed into the product $S$ having volume $V^S$, density $D^S$, total mass $M^S$ and mass $M_i^S$ of the component $i$. From the mass ratio:

$$K_i = \frac{M_i^S}{M_i^R} \qquad (3)$$

we define the relative mass change of the component $i$:

$$K_i - 1 = \frac{M_i^S}{M_i^R} - 1 = \Delta M_i / M_i^R \qquad (4)$$

A value of $K_i - 1 = 0$ (or $K_i = 1$) indicates that, during the transformation, the component $i$ does not change its mass: it behaves as an immobile component; for $K_i - 1 \neq 0$ (or $K_i \neq 1$), the component is mobile: $K_i - 1 < 0$ (or $K_i < 1$) and $K_i - 1 > 0$ (or $K_i > 1$) indicate loss and gain respectively. However, since each value of $K_i$ will be affected by the analytical error $\sigma K_i$, the component is here conventionally classified as immobile when $|K_i - 1| \leqslant \sigma K_i$, and mobile when $|K_i - 1| > \sigma K_i$.

Taking into account that $M = DV$ and that $M_i = MC_i$, where $C_i$ is the concentration of component $i$, substituting into (4) we obtain

$$K_i = \frac{M^S C_i^S}{M^R C_i^R} = \frac{V^S D^S C_i^S}{V^R D^R C_i^R} \qquad (5)$$

If the transformation of the rock occurs at constant volume (Gardner *et al.*, 1978; Gardner, 1980), the values of the intensive parameters D and C are sufficient for the evaluation of the component mobility. $K_i$ may also be evaluated using the concentrations of an immobile component (Nesbitt, 1979; Chesworth *et al.*, 1981).

Considering the concentrations of the immobile component $a$ ($K_a = 1$ and $M^S/M^R = C_a^R/C_a^S$), from equation (5), for a generic component $i$ we can write

$$K_i = \frac{C_i^S C_a^R}{C_i^R C_a^S} \qquad (6)$$

According to equation (6), if the concentrations of the immobile component $a$ and the concentration of the component $i$ in $S$ and $R$ are known, the values of $K_i$ may be easily calculated. The problem now is the identification of an immobile component. Theoretically, the identification could be made if the physical-chemical conditions of the system during transformation, and the behaviour of the components under these conditions, are known; normally, however, this is not possible and thus the identification may be made on the basis of the following considerations.

From equation (5), for two component $i$ and $j$ we can write

$$\frac{K_i M^R}{M^S} = \frac{C_i^S}{C_i^R}, \qquad \frac{K_j M^R}{M^S} = \frac{C_j^S}{C_j^R};$$

and thus

$$C_i^S = \frac{K_i C_i^R}{K_j C_j^R} C_j^S \qquad (7)$$

As a definition, the components $i$ and $j$ exhibit the same geochemical behaviour if at any stage of transformation $K_i = K_j$. In this case, equation (7) represents a straight line with zero intercept and a slope equal to the ratio between the concentrations of $i$ and $j$ in $R$. This line, of course, also describes the behaviour of the components during the transformation also when they are immobile ($K_i = K_j = 1$).

*Evaluation of the component behaviour in the whole outcrop.* For a defined component $i$, the values of $K_i$ obtained from samples of soil/saprolite collected in different places of the outcrop generally will be different because of the expected variable degree of alteration. Taking into account this finding, the minimum value of 68% of the samples with

$|K_i - 1| > \sigma K_i$ has been conventionally chosen as a limit for defining the prevalently mobile behaviour of the component $i$ in the whole altered system; the minimum value of 50% for defining the tendentially mobile behaviour. In other words, if 68% or more of the samples exhibit $|K_i - 1| > \sigma K_i$, the component has been considered as prevalently mobile at the scale of the whole outcrop; if only 50–67.9% have this characteristic, the component has been considered as tendentially mobile. Similarly, on the basis of $|K_i - 1| \leqslant \sigma K_i$, we define the prevalently immobile and the tendentially immobile behaviour.

The increasing shifting of the average of the $K_i$ values ($\overline{K_i}$) from the unit (toward zero and toward infinite for component loss or gain respectively) indicates increasing average degree of mobility of the component $i$. An order of increasing mobility would be defined only for components with the same sign of $\overline{K_i}$.

If the analytical error on $K_i$ is zero, the $SK_i/\overline{K_i}$ ratio (where $SK_i$ represents the standard deviation of the $K_i$ values) is an estimation of the degree of heterogeneity of the component behaviour in the investigated system during the alteration processes. As, however, $K_i$ is affected by analytical error, we have conventionally assumed $(SK_i - \overline{\sigma K_i})/\overline{K_i}$ (where $\overline{\sigma K_i}$ is the average standard error) as an approximate estimation of the degree of heterogeneity.

## Chemistry of the weathering

*Component behaviour at Mt. Prinzera.* Some ultramafic rocks, the strongly oxidized ultramafic breccia and several portions of weathering products sampled at the different stations (Table 3) have been analysed for major and trace elements. Representative analyses of soil/saprolite are reported in Table 4, whereas a complete list of the data (41 analyses of weathered samples) may be requested from the authors. The strongly oxidized breccia (sample PR027A) is not considered in the following discussion.

Disregarding the strongly oxidized breccia, the ultramafic outcrop may be considered as petrographically homogeneous. Nevertheless, because of the grain size (up to about 1 cm) of the rock and the presence of foliation and veins, three large samples (some kg) collected in different places have been analysed to check the chemical homegeneity of the outcrop. The average chemical composition is reported in Table 4. With the exception of CaO, all the components used for mass-balance calculation exhibit intervals around the obtained average values which are comparable to the analytical errors reported in Table 4 (for CaO the value is about three times the analytical error).

The meteoric waters penetrating into and collected in the ultramafic rocks of Mt. Prinzera feed some perennial and ephemeral springs which exhibit pH in the range 7.5–9; on the other hand, the 'standard' pH of the soil is in the range 6.4–7.8, the rain in the approximate range 4.2–7, and the biological activity very low to moderate. Under these conditions, the aluminium and titanium species are scarcely mobile because of the stability of Al- and Ti-bearing low-temperature silicates and hydoxides; for instance, for pH in the range 5–9, at 25°C the concentration of total Al in solution in equilibrium with gibbsite or kaolinite (assuming activity of $H_4SiO_4 \approx 10^{-5}$) is about $\leqslant 10^{-5}$ mole $Kg^{-1}$ and total Ti in equilibrium with $TiO(OH)_2$ is about $\leqslant 10^{-9}$ mole $Kg^{-1}$. Thus we can expect that Al and Ti behave as practically immobile components during the weathering. Actually, at Mt. Prinzera $Al_2O_3$ and $TiO_2$ exhibit high correlation coefficients (r = 0.95 and linear equation $Al_2O_3(\pm 0.66) = 21.68\ (\pm 1.12) \times TiO_2 + 1.36$, samples PR27 excluded), and an interesting distribution with decreasing slope at high $TiO_2$ values. The high value of the intercept on the y-axis decreases drastically when only samples with $TiO_2 <$ 0.30 wt.% are considered: the correlation coefficient remains high (0.95), the line practically passes for the origin (equation $Al_2O_3(\pm 0.59) = 27.25(\pm 1.71) \times TiO_2 + 0.40$) and the slope is very close to the $Al_2O_3/TiO_2$ ratio of the ultramafic protolith ($\approx$ 32; Table 4, PR01–10). This result indicates that for $TiO_2$ lower than about 0.3 wt.% we can approximately assume the same geochemical behaviour for $TiO_2$ and $Al_2O_3$ ($K_{TiO_2} = K_{Al_2O_3}$). Taking into account the strong difference in mineralogy between *R* and *S*, the general crystal-chemical features of the clay minerals and low temperature Fe-hydroxides, and the different valence of Ti and Al, the preservation of the condition $K_{TiO_2} = K_{Al_2O_3}$ (cf. relation 7) during increasing weathering should be really improbable in a case where the two components were both significantly mobilized. On the basis of all the previous considerations, we can assume that at least for $TiO_2$ contents less than about 0.30 wt.%, both $Al_2O_3$ and $TiO_2$ were not significantly mobilized; the apparent decrease of the $Al_2O_3/TiO_2$ ratio for $TiO_2 > 0.30$ wt.% could indicate increasing $Al_2O_3$ mobility as weathering increases. Thus $TiO_2$ has been practically assumed to be an immobile component for mass-balance calculations; by using the $TiO_2$ data for the weathered samples *S* and considering the average composition of the ultramafic rocks as representative of the starting serpentinite protolith (*R*, composition PR01–10, Table 4), values of $K_i$ for the other components have been estimated on the basis of relations (6).

In addition to the dominant effect of alteration, the $K_i$ values include the effects of (1) heterogeneity of

TABLE 4. Representative chemical analyses of ultramafic rocks and weathering products

| | | $SiO_2$ | $TiO_2$ | $Al_2O_3$ | $Fe_2O_3t$ | MnO | MgO | CaO | $Na_2O$ | $K_2O$ | $P_2O_5$ | LOI | Cr | Ni | Co | V | Cu | Zn | Sr | Ga | Zr |
|---|---|---|---|---|---|---|---|---|---|---|---|---|---|---|---|---|---|---|---|---|---|
| Standard error(σ) | | 0.40 | 0.015 | 0.2 | 0.35 | 0.02 | 0.35 | 0.1 | | | | 0.25 | 200 | 125 | 10 | 5 | 3 | 9 | 2 | 1 | 3 |
| Ultramafite | | | | | | | | | | | | | | | | | | | | | |
| PR01–10 | | 40.08 | 0.09 | 2.88 | 8.36 | 0.12 | 35.50 | 1.73 | <0.3 | <0.10 | <0.02 | 10.87 | 2463 | 2021 | 101 | 67 | 15 | 54 | 9 | 2 | 13 |
| Soil/saprolite | | | | | | | | | | | | | | | | | | | | | |
| Station 1 | | | | | | | | | | | | | | | | | | | | | |
| PR021 | B | 38.89 | 0.11 | 3.45 | 10.11 | 0.18 | 30.74 | 0.43 | <0.30 | <0.10 | 0.03 | 15.35 | 2864 | 2330 | 144 | 69 | 21 | 62 | 9 | 2 | 18 |
| PR020 | C | 40.39 | 0.08 | 2.59 | 9.69 | 0.19 | 32.69 | 0.27 | <0.30 | <0.10 | 0.02 | 13.72 | 2808 | 2638 | 118 | 61 | 15 | 51 | 5 | 2 | 11 |
| Station 2 | | | | | | | | | | | | | | | | | | | | | |
| PR19 | A | 38.73 | 0.21 | 5.61 | 11.21 | 0.19 | 27.47 | 0.91 | <0.30 | 0.10 | 0.04 | 15.06 | 4002 | 2247 | 150 | 106 | 19 | 85 | 13 | 5 | 26 |
| PR18(1) | A | 39.86 | 0.22 | 5.98 | 12.24 | 0.20 | 26.83 | 0.88 | <0.30 | 0.08 | 0.04 | 13.43 | 4319 | 2524 | 162 | 113 | 18 | 69 | 12 | 4 | 27 |
| PR17 | B | 41.12 | 0.26 | 7.20 | 13.35 | 0.22 | 24.93 | 1.01 | <0.30 | 0.12 | 0.03 | 11.55 | 4871 | 2600 | 166 | 122 | 24 | 80 | 13 | 6 | 36 |
| Station 3 | | | | | | | | | | | | | | | | | | | | | |
| PR16(1) | A | 42.49 | 0.26 | 6.72 | 11.51 | 0.19 | 25.65 | 0.41 | <0.30 | 0.24 | 0.02 | 12.26 | 2723 | 2342 | 124 | 82 | 35 | 85 | 24 | 7 | 35 |
| PR15 | B | 44.68 | 0.28 | 7.70 | 15.42 | 0.23 | 18.63 | 0.67 | <0.30 | 0.27 | 0.03 | 11.84 | 5055 | 2730 | 178 | 115 | 57 | 91 | 24 | 8 | 37 |
| PR14 | C | 47.30 | 0.38 | 9.52 | 11.10 | 0.18 | 19.80 | 0.28 | <0.30 | 0.24 | <0.02 | 11.14 | 2381 | 2351 | 89 | 87 | 34 | 100 | 7 | 10 | 59 |
| Station 4 | | | | | | | | | | | | | | | | | | | | | |
| PR47 | A | 39.76 | 0.24 | 6.44 | 11.03 | 0.18 | 23.72 | 0.68 | <0.30 | 0.31 | 0.05 | 16.23 | 3686 | 2063 | 149 | 104 | 23 | 87 | 18 | 7 | 37 |
| PR46 | B | 39.89 | 0.30 | 7.23 | 13.72 | 0.23 | 22.34 | 0.62 | <0.30 | 0.33 | 0.06 | 14.89 | 4478 | 2245 | 187 | 129 | 25 | 94 | 24 | 8 | 41 |
| PR45 | C | 40.50 | 0.11 | 4.00 | 12.23 | 0.16 | 28.22 | 0.22 | <0.30 | 0.08 | 0.03 | 13.56 | 2758 | 2400 | 142 | 80 | 24 | 62 | 4 | 2 | 4 |
| Station 5 | | | | | | | | | | | | | | | | | | | | | |
| PR51 | A | 35.96 | 0.14 | 4.06 | 10.83 | 0.16 | 27.78 | 0.44 | <0.30 | 0.10 | 0.10 | 19.45 | 3239 | 1911 | 135 | 99 | 22 | 84 | 14 | 4 | 18 |
| PR50 | B | 36.41 | 0.15 | 4.80 | 13.41 | 0.19 | 27.44 | 0.29 | <0.30 | 0.11 | 0.12 | 16.30 | 4155 | 2225 | 161 | 117 | 25 | 80 | 13 | 3 | 17 |
| Station 6 | | | | | | | | | | | | | | | | | | | | | |
| PR54 | A | 39.32 | 0.37 | 9.31 | 15.70 | 0.24 | 16.12 | 0.90 | 0.33 | 0.52 | 0.12 | 17.30 | 4084 | 1874 | 177 | 156 | 27 | 110 | 39 | 9 | 68 |
| PR53 | B | 39.45 | 0.32 | 8.61 | 16.13 | 0.23 | 19.35 | 0.66 | 0.24 | 0.42 | 0.10 | 14.57 | 4178 | 2211 | 173 | 150 | 26 | 98 | 32 | 9 | 56 |
| PR52 | C | 38.77 | 0.23 | 7.13 | 16.26 | 0.21 | 22.36 | 0.38 | <0.3 | 0.24 | 0.07 | 13.92 | 4359 | 2415 | 166 | 144 | 31 | 86 | 17 | 7 | 30 |
| Station 7 | | | | | | | | | | | | | | | | | | | | | |
| PR60 | B | 41.07 | 0.37 | 8.91 | 15.18 | 0.23 | 20.32 | 0.75 | 0.33 | 0.54 | 0.08 | 12.19 | 5114 | 2516 | 183 | 151 | 25 | 103 | 40 | 9 | 88 |
| PR61 | C | 40.37 | 0.31 | 8.02 | 14.41 | 0.20 | 22.63 | 0.64 | 0.26 | 0.47 | 0.08 | 12.38 | 4635 | 2523 | 173 | 160 | 25 | 95 | 34 | 7 | 71 |
| Station 8 | | | | | | | | | | | | | | | | | | | | | |
| PR41 | A | 45.05 | 0.25 | 8.65 | 19.50 | 0.21 | 14.52 | 0.68 | <0.30 | 0.24 | <0.02 | 10.92 | 4761 | 3051 | 158 | 115 | 47 | 95 | 12 | 9 | 30 |
| PR55 | B | 45.90 | 0.26 | 7.13 | 17.51 | 0.26 | 20.44 | 1.12 | <0.30 | <0.10 | <0.02 | 7.99 | 4037 | 3257 | 198 | 88 | 45 | 86 | 6 | 7 | 14 |
| PR56 | C | 41.83 | 0.27 | 7.33 | 13.23 | 0.20 | 22.54 | 1.15 | <0.30 | <0.10 | <0.02 | 13.21 | 2990 | 2561 | 123 | 70 | 36 | 59 | 7 | 6 | 20 |
| Station 9 | | | | | | | | | | | | | | | | | | | | | |
| PR59 | A | 42.83 | 0.21 | 7.43 | 19.21 | 0.20 | 14.22 | 0.59 | <0.30 | 0.13 | <0.02 | 15.05 | 5086 | 3034 | 166 | 101 | 48 | 97 | 8 | 7 | 21 |
| PR58(1) | B | 43.18 | 0.41 | 9.41 | 15.01 | 0.27 | 17.44 | 1.77 | 0.38 | 0.46 | 0.05 | 11.93 | 5269 | 2211 | 201 | 145 | 33 | 108 | 37 | 10 | 85 |
| PR57 | C | 41.65 | 0.28 | 8.32 | 22.11 | 0.28 | 14.76 | 0.52 | <0.30 | 0.24 | 0.03 | 11.97 | 4339 | 4005 | 198 | 116 | 55 | 103 | 16 | 10 | 31 |
| Station 10 | | | | | | | | | | | | | | | | | | | | | |
| PR27 | A | 38.62 | 0.27 | 8.37 | 20.46 | 0.27 | 16.99 | 1.97 | <0.30 | 0.13 | 0.05 | 12.50 | 7108 | 3198 | 262 | 196 | 37 | 279 | 13 | 6 | 22 |

X-ray fluorescence analyses obtained on samples dried at 100°C: oxides in wt.% and elements in ppm. $Fe_2O_3t$ = total iron as $Fe_2O_3$. LOI = loss on ignition in the range 100–1050°C.

the original ultramafic protolith, (2) addition of small amounts of allogenic minerals, and (3) analytical error on $K_i$. All these effects increase the scattering of the $K_i$ data. Concerning point (2), we can reasonably state that the $TiO_2$ distribution is not significantly influenced by Ti-bearing allogenic minerals since their occurrence is only occasional.

It is apparent from Table 5 that, at the scale of the whole outcrop, Ca, Mg, Si, Ni and Co are prevalently mobile, as more than 68% of the analysed samples exhibit $|K_i - 1| > \sigma K_i$, whereas Zn, V, Fe, Cr and Mn are only tendentially mobile. The average negative balance for all these components at the scale of the whole outcrop is indicated by $\overline{K_i} < 1$; the average degree of mobility, which increases as $\overline{K_i}$ decreases, follows the order Ca > Mg > Si > Ni > Co $\approx$ Zn $\approx$ V > Fe = Cr $\approx$ Mn. A high loss of Mg, Si and Ca also characterizes other ultramafic areas, such as the saprolite of Tagaung Taung, Burma (Shellmann, 1989*b*); however, in contrast with Mt. Prinzera, at Tagaunn Taung Cr is considered immobile and Ni is very enriched ($K_{Ni} \approx 2.5$) because of a contribution from an overlying limonite layer. In spite of the addition of allogenic quartz, with the exception of only three samples, the silica balance is always strongly negative as expected in a system where quartz is apparently unstable. The elements Al, Ga, Zr and, of course, Ti are prevalently immobile as frequently occurs during epigenetic and metamorphic processes (Ti and Zr: Law *et al.*, 1991; Pearce and Cann, 1973). As these elements are practically immobile, they do not exhibit heterogeneity of their behaviour during the weathering in the different portions of the outcrop, i.e. for them $(SK_i - \overline{\sigma K_i})/\overline{K_i} \leqslant 0$ (Table 5). On the contrary, with the exception of Ca, the most mobile elements Mg, Si and Ni show the highest degree of heterogeneity. This may be mostly referred to a variable degree of transformation of the original protolith at the different sites and at the different depths in the same profile. The absence of heterogeneity for Ca together with the high mobility of this element indicate that the Ca-bearing minerals (clinopyroxene, calcite) are easily dissolved everywhere.

*Mass removed.* From equation (5), the relative total mass change proceeding from *R* to *S* may be calculated using an immobile component *a* (in our case *a* is $TiO_2$):

$$\frac{\Delta M}{M^R} = \frac{M^S}{M^R} - 1 = \frac{C_a^R}{C_a^S} - 1 \qquad (8)$$

At Mt. Prinzera, the resulting $100 \times \Delta M/M^R$ value is largely variable for the different samples, but, on average, very low ($-52 \pm 28$, average $\pm$ standard deviation) indicating a strong loss of mass during alteration. The contribution of the different components to the amount of the chemically removed material may be evaluated according to the following equation obtained from relation (4):

$$\frac{\Delta M_i}{M^R} = C_i^R(K_i - 1) \qquad (9)$$

The results indicate that, among the prevalently to tendentially mobile components listed in Table 5, the highest contribution to mass loss is due to Si and Mg, whereas the other elements played a secondary role contributing only up to some few per cent. For convenience of the reader, the average mass loss [expressed as (gms of the element)/(kg of total mass)] for prevalently to tendentially mobile components is reported in Table 5. Moreover, as indicated by the value $(C_i^S/C_i^R) - 1$ (= average relative variation of the concentration, where $C_i^S$ is the average concentration in the whole altered system; Table 5), the removal of the mass led to a decrease in the average concentrations of Mg and Ca, and to an increase of all the other elements with the exception of Si which, on average, practically maintains its original concentration.

*Water–rock chemical relationships.* Water penetrating the soil/saprolite and the ultramafic substratum reasonably was and is responsible for the element mobility. Analyses of perennial and ephemeral springs of Mt. Prinzera (Table 6) demonstrated that the concentration ratios of the components analysed in the waters are qualitatively in agreement with the mobility of the components discussed above. Consider for instance, Mg, Ca and Cr. According to the results summarized in Table 5, the average degree of mobility of these elements is in the order Cr < Mg < Ca; thus, assuming that the rain consists only of pure water, using concentrations in the ultramafic rocks *R* and in the spring waters *W*, we would expect $(Cr^R/Cr^W) > (Mg^R/Mg^W) > (Ca^R/Ca^W)$: values actually found are $(Cr^R/Cr^W) \times 10^{-4} = 12-14$, $(Mg^R/Mg^W) \times 10^{-4} = 0.54-0.59$ and $(Ca^R/Ca^W) \times 10^{-4} = 0.07-0.14$ (the ephemeral spring 9 has not been considered because it is not representative of the dominant leaching process). This relationship does not change considering the actual rain which contains low Ca and Mg (<2.2 and <0.6 mg/kg respectively; G. Curti, pers. comm., 1995).

The degree of saturation in calcite, chrysotile, talc and brucite in the analysed waters is expressed by the saturation index S.I. = $\log_{10}(Q/K)$, where K is the equilibrium constant for the dissolution reactions and Q the actual activity product of the components. The S.I.values (Table 6) have been calculated from the activities obtained using the water speciation program of Ball and Nordstrom (1992). In agreement with the absence of brucite in the investigated outcrop, all the waters are under-

TABLE 5. Geochemical behaviour of some components during the weathering

| | Si | Al | Fe | Mn | Mg | Ca | Cr | Ni | Co | V | Cu | Zn | Sr | Ga | Zr |
|---|---|---|---|---|---|---|---|---|---|---|---|---|---|---|---|
| $\overline{K_i}$ | 0.49 | 0.89 | 0.73 | 0.74 | 0.36 | 0.17 | 0.73 | 0.60 | 0.67 | 0.69 | 0.92 | 0.68 | 0.65 | 1.13 | 0.94 |
| $SK_i$ | 0.27 | 0.11 | 0.28 | 0.31 | 0.30 | 0.07 | 0.30 | 0.34 | 0.28 | 0.20 | 0.40 | 0.23 | 0.25 | 0.22 | 0.30 |
| $(\overline{SK_i} - \overline{\sigma K_i})/\overline{K_i}$ | 0.23 | $\leqslant 0$ | 0.06 | $\leqslant 0$ | 0.52 | $\leqslant 0$ | 0.02 | 0.17 | $\leqslant 0$ | $\leqslant 0$ | $\leqslant 0$ | $\leqslant 0$ | $\leqslant 0$ | $\leqslant 0$ | $\leqslant 0$ |
| $(\overline{C_i^S}/C_i^R) - 1$ | 0.02 | 1.21 | 0.63 | 0.65 | −0.32 | −0.58 | 0.61 | 0.25 | 0.49 | 0.59 | 1.09 | 0.54 | 0.73 | 1.93 | 1.53 |
| Classification groups | | | | | | | | | | | | | | | |
| | Per cent of samples | | | | | | | | | | | | | | |
| immobile | | | | | | | | | | | | | | | |
| $\lvert K_i - 1\rvert \leqslant \sigma K_i$ | 12.8 | 89.7 | 35.9 | 48.7 | 7.7 | | 41.0 | 17.9 | 28.2 | 33.3 | 61.5 | 43.6 | 51.3 | 100.0 | 87.2 |
| mobile | | | | | | | | | | | | | | | |
| $\lvert K_i - 1\rvert > \sigma K_i$ | 87.2 | 10.3 | 64.1 | 51.3 | 92.3 | 100.0 | 59.0 | 82.1 | 71.8 | 66.7 | 38.5 | 56.4 | 48.7 | | 12.8 |
| | Mass removed (gm of element/kg of total mass) | | | | | | | | | | | | | | |
| | 96 | | 16 | <0.5 | 136 | 10 | 0.67 | 0.81 | <0.5 | < 0.5 | | <0.5 | | | |

$\overline{K_i}$ = average of the $K_i$ values obtained according to the relation (6) of the text and assuming $TiO_2$ as immobile component; $C_i$ = concentration of a generic component; $S$ = soil/saprolite, $R$ = ultramafite reported in Table 4; $SK_i$ = standard deviation for $K_i$; $(\overline{C_i}/C_i^R) - 1$ = average of the relative variation of the component concentration (for $TiO_2$, the value not reported on the Table is 1.56); $\sigma K_i$ = standard error on $K_i$ calculated according to the relation $(\sigma K_i/K_i) = (\sigma_i^S/C_i^S) + (\sigma_{TiO_2}^S/C_{TiO_2}^S) + (\sigma_i^R/C_i^R) + (\sigma_{TiO_2}^R/C_{TiO_2}^R)$, where $\sigma^S$ are values of the standard analytical errors reported in Table 4 for the different components and $\sigma^R$ are the uncertainties on the reference ultramafic composition due to the heterogeneity of the ultramafic rocks as discussed in the text; the uncertainties on the reference ultramafic composition are considered equal to the analytical standard errors for all the components with the exception of CaO for which we have assumed $\sigma_{CaO}^R = 0.3$; $\overline{\sigma K_i}$ = average value of the standard error on $K_i$. Per cent of samples: the values are percentages of analysed samples showing the same behaviour (samples 27A excluded) (see text for further explanation). Mass removed = average amounts (grams) of prevalently to tendentially mobile components chemically removed during the alteration from one kg of original serpentinite.

TABLE 6. Chemical composition of spring waters

| Spring number | 1 | | 8 | | 9 | |
|---|---|---|---|---|---|---|
| | mg/kg | Analytical molality × $10^5$ | mg/kg | Analytical molality × $10^5$ | mg/kg | Analytical molality × $10^5$ |
| Na | 1.2 | 5.2 | 4.2 | 18 | 1.1 | 4.8 |
| K | | | | | 0.6 | 1.5 |
| Ca | 8.7 | 21.7 | 17.3 | 43.2 | 3.5 | 8.7 |
| Mg | 39.7 | 163 | 36.4 | 150 | 23.0 | 95 |
| $HCO_3$(T) | 175 | 287 | 181 | 297 | 99 | 162 |
| Cl | 4.0 | 11 | 4.9 | 14 | 4.4 | 12 |
| $NO_3$ | | | 0.3 | 0.5 | 8.8 | 14 |
| $SO_4$ | 38.2 | 39.8 | 46.9 | 48.8 | 16.7 | 17.4 |
| | µg/kg | | µg/kg | | µg/kg | |
| Pb | 1.0 | | 1.0 | | 2.0 | |
| Cr | 18.0 | | 20.0 | | 18.0 | |
| Cd | 0.2 | | | | 1.0 | |
| pH | 9.0 | | 8.0 | | 8.0 | |
| T(°C) | 11.5 | | 11.3 | | 12.8 | |
| E.I.S. | | 0.0056 | | 0.0061 | | 0.0033 |

| Spring number<br>Saturation index at 1 bar and 12°C for: | | 1<br>logQ/K | 8<br>logQ/K | 9<br>logQ/K |
|---|---|---|---|---|
| calcite | logK = −8.42 ± 0.02 (1σ) | 0.46 | −0.15 | −1.0 |
| chrysotile | = 33.90 | < 2.90 | < −3.22 | < −3.68 |
| talc | = 22.95 ± 2.00 (1σ) | < 5.46 | < −0.63 | < −1.09 |
| brucite | = 17.75 | −2.70 | −4.73 | −4.89 |

1 and 8 = perennial springs; 9 = ephemeral spring. Fe ⩽ 0.01 mg/kg, $NH_4$ < 0.01 mg/kg, $NO_2$ < 0.003 mg/kg. $HCO_3$(T) = carbonate alkalinity espressed as $HCO_3$. E.I.S. = effective ionic strength calculated on the basis of the solute speciation results (Ball and Nordstrom, 1992). Saturation index = $\log_{10}Q/K$, where K is the equilibrium constant for the following dissolution reactions and Q the activity product of the involved components as deduced from speciation calculation (Ball and Nordstrom, 1992): $CaCO_{3(calcite)} = Ca^{2+}_{aq} + CO^{2-}_{3(aq)}$; $Mg_3Si_2O_5(OH)_{4(chrysotile)} + 6H^+_{aq} = 3Mg^{2+}_{aq} + 2H_4SiO_{4(aq)} + H_2O$, activity of chrysotile component = 0.94 in rough agreement with the composition reported in Table 2; $Mg_3Si_4O_{10}(OH)_{2(talc)} + 4H_2O + 6H^+_{aq} = 3Mg^{2+}_{aq} + 4H_4SiO_{4(aq)}$; $Mg(OH)_{2(brucite)} + 2H^+_{aq} = Mg^{2+}_{aq} + 2H_2O$. The values of $\log_{10}Q/K$ reported for chrysotile and talc are upper limits calculated assuming water in equilibrium with quartz, i.e. activity of $H_4SiO_{4(aq)} = 10^{-4.2}$.

saturated in brucite. Spring 8, which is representative of the most common waters at Mt. Prinzera, and spring 9, are undersaturated in calcite, whereas spring 1 is saturated. Springs 8 and 9 could be theoretically saturated in talc and spring 1 both in talc and chrysotile if the activity of $H_4SiO_4$ is appropriate. The apparent absence of talc in the whole outcrop imposes an upper limit for $\log_{10} a^{aq}_{H_4SiO_4}$; however, because of the high uncertainty on $\log_{10} K_{talc}$, this limit ($\log_{10} a^{aq}_{H_4SiO_4} < -5.5 \pm 2.0$, 1σ) cannot be considered significantly different from that imposed by quartz instability ($\log_{10} a^{aq}_{H_4SiO_4} < -4.2$).

## Summary and conclusions

(1) The saprolite/soil which covers the Mt. Prinzera serpentinites consists of: (i) weathering phases, mostly smectite and Fe-oxides/hydroxides; (ii) relics of serpentinite, mostly lizardite and minor chlorite and chrysotile; (iii) pre-serpentinization phases including spinel, pyroxenes and olivine; (iv) a small quantity of allogenic minerals such as quartz and K-feldspar, and exceptional biotite and zircon. Quartz, K-feldspar, biotite and zircon were probably accumulated by aeolian transport or surface water from surrounding and/or areas further afield.

(2) The chemical mobility of the elements during weathering has been estimated considering $TiO_2$ as a practically immobile component. Most of the elements were removed in variable amounts during weathering; the average degree of mobility follows the order Ca > Mg > Si > Ni > Co ≈ Zn ≈ V > Fe = Cr ≈ Mn. This behaviour reflects the balanced effect of the rate of dissolution of the serpentinite minerals, the crystal-chemical features of the new-forming phases and the absorption processes, which have been not investigated in this paper. The weathering led to an average increase of the relative concentration of most elements, in the order Ga, Ti, Zr, Al ≫ Sr > Mn, Fe, Cr, V > Zn, Co > Ni, and to a decrease in the concentration of Ca and Mg.

(3) The the relative mass change of the serpentinite protolith during chemical weathering was very high (on average about 52%). The highest contribution to the mass loss was by Si and Mg.

(4) At least for Cr, Mg and Ca, the composition of perennial and ephemeral springs is in agreement with the element mobility as deduced from the mass-balance calculations.

## Acknowledgements

We are grateful to A. Basu (Bloomington), G. Mezzadri, G. Rossetti and E. Salvioli Mariani (Parma), to D.H.M. Alderton (London) and to the kind anonymous referee for the useful suggestions and support; to G. Curti (Presidio Multizonale di Prevenzione, Parma), M.G. Brigatti and L. Poppi (Modena) for general information. The CNR, National Research Council, Rome, is also acknowledged for financial support (grants 94.00188.CT05 and 95.00361.CT05).

## References

Ball, J.W. and Nordstrom, D.K. (1992) User's manual for WATEQ4F, with revised thermodynamic data base and test cases for calculating speciation of major, trace, and redox elements in natural waters. *U.S. Geological Survey, Open-File Report 91–183*, Denver, Colorado.

Barnes, I. and O'Neil, J.R. (1969) The relationship between fluids in some fresh alpine-type ultramafics and possible modern serpentinization, Western United States. *Geol. Soc. Amer. Bull.*, **80**, 1947–60.

Beccaluva, L., Emiliani, F., Venturelli, G. and Zerbi M. (1973) Ca, Fe, Mg, Mn, Cr, Ni, Co distribution in some ultramafic rocks outcropping it the Northern Apennines with some geological remarks. *Ateneo Parmense-Acta Naturalia (Parma)*, **9**, 69–98.

Berner, R.A. (1981) Kinetics of weathering and diagenesis. In *Kinetics of Gechemical Processes* (A.C. Lasaga and R.J. Kirkpatrick, eds.), *Reviews in Mineralogy*, **8**, Mineral. Soc. America, 1981, pp.111–34.

Chesworth, W., Dejou, J. and Larroque, P. (1981) The weathering of basalt and relative mobilities of the major elements at Belbex, France. *Geochim. Cosmochim. Acta*, **45**, 1235–43.

Cleaves, E.T., Fisher, D.W. and Bricker, O.P. (1974) Chemical weathering of serpentinite in the eastern Piedmont of Maryland. *Geol. Soc. Amer. Bull.*, **85**, 437–44.

Cortesogno, L., Mazzucotelli, A. and Vannucci, R. (1979) Some examples of pedogenesis on ultramafic rocks in Mediterranean climate (in Italian). *Ofioliti*, **4**, 295–312.

Drees, L.R., Wilding, L.P., Smeck, N.E. and Senkayi, A.L. (1989) Silica in soils: quartz and disordered silica polimorphs. In *Minerals in Soil Environment*, 2nd ed., Soil Science Soc. Amer., Madison, pp. 913–74.

Enüstün, B.V. and Turchevich, J. (1960) Solubility of fine particles of strontium sulfate. *J. Amer. Chem. Soc.*, **82**, 4502–9.

Gardner, L.R. (1980) Mobilization of Al and Ti during weathering - Isovolumetric geochemical evidence. *Chem. Geol.*, **30**, 151–65.

Gardner, L.R., Kheorueromne, I. and Chen, H.S. (1978) Isovolumetric geochemical investigation of a buried granite saprolite near Columbia, SC, U.S.A. *Geochim. Cosmochim. Acta*, **42**, 417–24.

Hey, M.H. (1954) A new review of the chlorites. *Mineral. Mag.*, **30**, 277–92.

Law K.R., Nesbitt H.W. and Longstaffe F.J. (1991) Weathering of granitic tills and the genesis of a podzol. *Amer. J. Sci.*, **291**, 940–76.

Mazzullo, J., Ehrlich, R. and Hemming, M.A. (1984) Provenance and areal distribution of late Pleistocene and Holocene quartz sand on the Southern New England continental shelf. *J. Sedim. Petrol.*, **54**, 1335–1348.

Minguzzi, V., Morandi, N. and Nannetti, M.C. (1985) Mineralogy and geochemistry of soils occurring on the Serra del Zanchetto ophiolite (Bologna) (in Italian). *Mineral. Petrog. Acta (Bologna)*, **29A**, 145–63.

Nahon, D.B. and Colin, F. (1982) Chemical weathering of orthopyroxenes under lateritic conditions. *Amer. J. Sci.*, **282**, 1232–43.

Nesbitt, H.W. (1979) Mobility and fractionation of rare earth elements during weathering of a granodiorite. *Nature*, **279**, 206–10.

Nielsen, A.E. (1964) *Kinetics of Precipitation*. Pergamon Press, Oxford.

Parks, G.A. (1984) Surface and interfacial free energies of quartz. *J. Geophys. Res.*, **89**, 3997–4008.

Pearce, A.J. and Cann, J.R. (1973) Tectonic setting of basic volcanic rocks determined using trace element analyses. *Earth Planet. Sci. Lett.*, **19**, 290–300.

Piccardo, G.B., Rampone, E. and Vannucci, R. (1990) Upper mantle evolution during continental rifting and ocean formation: evidences from peridotite bodies of the Western Alpine- Northern Apennines system. *Mem. Soc. Géol. France*, **156**, 323–33.

Pittman, E.D. (1972) Diagenesis of quartz in sandstones as revealed by scanning electron microscopy. *J. Sedim. Petrol.*, **42**, 507–19.

Rampone, E., Piccardo, G.B., Vannucci, R., Bottazzi, P. and Ottolini, L. (1993) Subsolidus reaction monitored by trace element partitioning: the spinel- to plagioclase- facies transition in mantle peridotites. *Contrib. Mineral. Petrol.*, **115**, 1–17.

Shellmann, W. (1989*a*) Allochthonous surface alteration of Ni-laterites. *Chem. Geol.*, **74**, 351–64.

Shellmann, W. (1989*b*) Composition and origin of lateritic nickel ore at Tagaung Taung, Burma. *Mineral. Deposita*, **24**, 161–8.

Stumm, W. and Morgan, J.J. (1981) *Aquatic Chemistry*. 2nd ed., Wiley-Interscienes, New York.

Thorez, J. (1976) *Practical Identification of Clay Minerals*. Lelotte, Dison.

Wildman, W.E., Whittig, L.D. and Jackson, M.L. (1971) Serpentine stability in relation to formation of iron-rich montmorillonite in some California soils. *Amer. Mineral.*, **56**, 587–602.

Wilson, M.J. and Berrow, M.L. (1978) The mineralogy and heavy metal content of some serpentinite soils in North-East Scotland. *Chem. Erde*, **37**, 181–205.

Yusta, A., Barahona, E., Huertas, F., Reyes, E., Yanez, J. and Linares, J. (1985) Geochemistry of soils from peridotites in Los Reales, Malaga, Spain. *Miner. Petrogr. Acta (Bologna)*, **29A**, 489–98.

[*Manuscript received 27 August 1996: revised 17 March 1997*]